Evaluating Origin of Electron Traps in Tris(8-hydroxyquinoline) Aluminum Thin Films using Thermally Stimulated Current Technique

Toshinori MATSUSHIMA[1] and Chihaya ADACHI[1,2]*

[1]*Core Research for Evolutional Science and Technology Program, Japan Science and Technology Agency, 1-32-12 Higashi, Shibuya, Tokyo 150-0011, Japan*

[2]*Center for Future Chemistry, Kyushu University, 744 Motooka, Nishi, Fukuoka 819-0395, Japan*

We measured the energy distributions and concentrations of electron traps in non-O_2-exposed and O_2-exposed tris(8-hydroxyquinoline) aluminum (Alq_3) films using a thermally stimulated current (TSC) technique to investigate how doping O_2 molecules in Alq_3 films affect the films' electron trap and electron transport characteristics. The results of our TSC studies revealed that Alq_3 films have an electron trap distribution with peak depths ranging from 0.075 to 0.1 eV and peak widths ranging from 0.06 and 0.07 eV. Exposing the Alq_3 films to O_2 atmosphere induced a marked increase in electron trap concentration, indicating that electron traps with an energy distribution originate from O_2 molecules absorbed in Alq_3 films. We measured the current

density-voltage characteristics of these films. The driving and turn-on voltages of the O_2-exposed Alq_3 film became higher than those of the O_2-unexposed Alq_3 film owing to the increase in electron trap concentration caused by the O_2 doping of the Alq_3 films.

KEYWORDS: tris(8-hydroxyquinoline) aluminum, electron trap, electron transport, thermally stimulated current, oxygen

*E-mail address: adachi@cstf.kyushu-u.ac.jp

1. Introduction

Carrier trapping is one of the most important factors that markedly minimize carrier transport in organic thin films.[1-6] Most organic light-emitting diodes (OLEDs) are typically composed of an organic hole-transporting layer (HTL), an emitting layer (EML), and an electron-transporting layer (ETL),[7-9] and have hole mobilities of HTLs that are higher than electron mobilities of ETLs.[3,4,10] The large difference in carrier mobility between HTLs and ETLs induces an imbalance in the numbers of injected holes and electrons in EMLs and an increase in the driving voltage in OLEDs, resulting in reduced electroluminescence efficiency of OLEDs.[11] The cause of the reduction in electron mobility may be the presence of a large density of electron traps in ETLs. In fact, marked reductions in field-effect[6] and time-of-flight (TOF) electron mobilities[3,4] have been observed in O_2-absorbed films of small organic molecules, suggesting that O_2 molecules potentially work as electron traps in organic films. An increase in carrier trap concentration has been observed in O_2-absorbed polymer films using a thermally stimulated current (TSC) technique.[12-14] Therefore, a detailed understanding of how O_2 molecules absorbed in organic films are related to electron traps is crucial for determining the underlying mechanisms of carrier transport in organic films and for improving OLED performance.

Tris(8-hydroxyquinoline) aluminum (Alq_3) is a material widely used as an ETL in OLEDs owing to its relatively high electron mobility and high thermal stability.[2-4,7-10] Therefore, we prepared Alq_3 films to investigate their electron trap and electron transport characteristics. Extensive research on electron trap and electron transport characteristics in Alq_3 films has been experimentally and theoretically conducted.[2-4,10,15-23] However, no direct observation or systematic investigation of the relationship between O_2 molecules absorbed in Alq_3 films, electron traps, and electron transport, has been reported to date. Therefore, we measured the energy distributions and concentrations of electron traps in O_2-exposed and O_2-unexposed Alq_3 films using a TSC technique. This technique is a powerful tool for characterizing carrier traps in small organic molecules,[15,23-25] polymers,[12-14] and inorganic materials.[26,27] We demonstrated that Alq_3 films have electron traps with an energy distribution that originate from O_2 molecules absorbed in the Alq_3 films and that these O_2 traps minimize electron transport in the Alq_3 films.

2. Experimental Methods

We fabricated Alq_3 single-layer devices with a glass substrate/MgAg anode layer (100 nm)/Alq_3 layer (100 nm)/MgAg cathode layer (100 nm) structure using the

following steps: Glass substrates with an area of 25 x 25 mm^2 were cleaned ultrasonically in a mixture of detergent (Cica clean *LX*-II, Kanto Chemicals) and pure water (1/10 by volume) for 10 min, followed by ultrasonication in pure water for 10 min, in acetone for 10 min, and in isopropanol for 10 min. The glass substrates were soaked in boiling isopropanol for 5 min and then placed in an ultraviolet-ozone treatment chamber (UV.TC.NA.003, Bioforce Nanoscience) for 20 min. The cleaned substrates were transferred to a vacuum evaporator, which was evacuated using a rotary mechanical pump and a turbo molecular pump. At a background pressure of 10^{-3} Pa, a 100-nm-thick MgAg (Mg/Ag = 10/1 by weight) alloy layer[7,8] was vacuum-deposited on the glass substrates at a deposition rate of 0.33 nm s^{-1} using two resistively heated tungsten boats through a shadow mask with striped openings to form a striped MgAg anode layer with a width of 2 mm. High-purity Alq_3 was obtained from Nippon Steel Chemical Co. and used as-received. A 100-nm-thick Alq_3 layer was vacuum-deposited on top of the MgAg anode layer at a deposition rate of 0.3 nm s^{-1} at a background pressure of 10^{-4} Pa using a resistively heated tantalum boat through the shadow mask with a square opening, whose area was larger than that of a shadow mask used to deposit the MgAg anode layer. We prepared these MgAg/Alq_3 layers on four different substrates under the same vacuum deposition conditions. All the Alq_3 layers prepared on

the different substrates were transferred to a nitrogen-filled glove box with oxygen and water concentrations less than 0.1 ppm without exposing them to air. Two of the four substrates were exposed to pure O_2 atmosphere for 1 min in a small metal chamber for the Alq_3 layers to absorb O_2, and the other two substrates were stored in a nitrogen-filled glove box to prevent the absorption of O_2 by the Alq_3 layers. To complete the devices, all the O_2-unexposed and O_2-exposed substrates were again transferred to a vacuum evaporator. At $\approx 10^{-3}$ Pa, a 100-nm-thick MgAg (Mg/Ag = 10/1 by weight) alloy layer[7,8] was vacuum-deposited on top of the Alq_3 layers at a deposition rate of 0.33 nm s^{-1} using two resistively heated tungsten boats through a shadow mask to form a striped MgAg cathode layer with a width of 2 mm. The striped MgAg anode and cathode layers were overlapped perpendicularly, indicating that the active areas of our Alq_3 devices were limited to be a 4 mm^2 area. The Alq_3 devices were covered with a glass cap using a moisture getter sheet (GDO, SAES Getters Japan) and ultraviolet curing epoxy resin (XNR5516-ZHV, Nagase Chemtex) inside a nitrogen-filled glove box. We used two O_2-unexposed and O_2-exposed substrates for TSC measurement and the remaining two O_2-unexposed and O_2-exposed substrates for the measurement of current density-voltage (*J*-*V*) characteristics.

We investigated the electron trap characteristics of the O_2-unexposed and

O_2-exposed Alq_3 films using the T_{START}-T_{STOP} TSC technique reported by Steiger *et al.*,[23] which is useful for characterizing the energy distribution and concentration of electron traps in organic films. The Alq_3 device was set in a TSC measurement chamber (TSC-FETT EL2000, Rigaku), and the MgAg anode and cathode layers were wired with gold leads. The TSC measurement chamber was evacuated using a rotary mechanical pump and then filled with He that acted as a heat transfer medium. These evacuation and filling procedures were repeated five times to replace the chamber with He completely. The device was cooled to 80 K, called T_{START}, using liquid nitrogen. At T_{START}, the device was biased with a constant current flow of 5 mA cm^{-2} for 1 min to charge electron traps with injected electrons from the MgAg cathode. Device temperature was increased to a temperature called T_{STOP}, which was higher than T_{START}, using a collecting bias of 0.5 V at a heating rate of 0.17 K s^{-1}. Dark current was confirmed to be negligible at this collecting bias over the entire temperature range from T_{START} to room temperature (T_{RT}). During this first temperature increase, electrons are partially released from traps. After reaching T_{STOP}, the device was cooled to T_{START} again. Then, the device was heated to T_{RT} using a collecting bias of 0.5 V at a heating rate of 0.17 K s^{-1} without electrical trap charging at T_{START}. During this second temperature increase, residual electrons were released from traps and collected using a

femtoammeter installed in our TSC system. We repeated these measurements using a higher T_{STOP} within the range from 80 to 160 K to investigate the dependence of T_{STOP} on TSC spectra. Details of this T_{START}-T_{STOP} TSC technique have been described by Stiger *et al*.[23] To compare electron trap and electron transport characteristics, the *J*-*V* characteristics of O_2-unexposed and O_2-exposed Alq_3 devices were measured using a semiconductor parameter analyzer (E5250A, Agilent Technologies Inc) at T_{RT}.

3. Results and Discussion

Figures 1(a) and 1(b) show the TSC vs sample temperature characteristics as functions of T_{STOP}, which were measured during the second temperature increase from T_{START} to T_{RT}, for the O_2-unexposed and O_2-exposed Alq_3 films, respectively. The areas of the TSC spectra gradually decreased as T_{STOP} was increased from 80 to 160 K because electrons were partially released from traps during the first temperature increase.[23] We found that the TSC of the O_2-exposed Alq_3 film was about one order of magnitude higher than that of the O_2-unexposed Alq_3 film, indicating that O_2-exposed Alq_3 films have a higher electron trap concentration than O_2-unexposed Alq_3 films.

Assuming that all electrons detrapped during the second temperature increase were collected by the MgAg electrodes and that they all contributed to TSC, the total electron

trap concentration (N_t) of the Alq_3 layers can be calculated using[6,26)]

$$N_t = \frac{Q}{qAL}, \quad (1)$$

where Q is the total charge, which is equal to the area under the TSC peak, q is the electronic charge, A is the active device area, and L is the cathode-anode spacing. From the TSC spectra measured at a T_{STOP} of 80 K shown in Figs. 1(a) and 1(b), the total electron trap concentrations were respectively calculated to be 7.3 x 10^{16} cm^{-3} for the O_2-unexposed Alq_3 films and 6.2 x 10^{17} cm^{-3} for the O_2-exposed Alq_3 films using eq. (1).

We replotted Figs. 1(a) and 1(b) as Arrhenius-type plots, that is, logarithmic TSC vs reciprocal sample temperature as functions of T_{STOP}, in Figs. 2(a) and 2(b), respectively. From the initial slopes of TSC (I_{TSC}) shown in Figs. 2(a) and 2(b), the activation energy (E_A) of electrons can be calculated using[15,23)]

$$I_{TSC} \propto \exp\left(\frac{-E_A}{kT}\right), \quad (2)$$

where k is Boltzmann's constant and T is the temperature. Fitting the experimental data with eq. (2) [the solid lines in Figs. 2(a) and 2(b)] provided activation energies ranging from 0.06 to 0.19 eV. The width of a Gaussian-type density-of-states (DOS) distribution in an Alq_3 film has been shown to be ≈0.1 eV.[18)] The activation energies we estimated (0.06-0.19 eV) were slightly larger than half the width of a DOS distribution in an Alq_3

film (≈0.05 eV), indicating that these activation energies correspond to the depths of electron traps lying below the DOS distribution of Alq_3.

The electron trap depth, corresponding to E_A, vs T_{STOP} characteristics of the O_2-unexposed and O_2-exposed Alq_3 films are shown in Figs. 3(a) and 3(b), respectively. The electron trap depths remained unchanged, regardless of T_{STOP}, in the T_{STOP} range from 80 to 100 K, as shown in Fig. 3(a), indicating that electron traps lie at a discrete energy level.[23] In contrast, electron trap depth markedly depended on T_{STOP} in the T_{STOP} range from 110 to 160 K, as shown in Fig. 3(a), and in the entire T_{STOP} range, as shown in Fig. 3(b), indicating that an electron trap distribution is formed in Alq_3 films.[23] These results suggest that the O_2-unexposed Alq_3 film has two types of electron traps: electron traps at a discrete energy level and electron traps with an energy distribution, in contrast, the O_2-exposed Alq_3 film has only electron traps with an energy distribution.

The electron trap concentration per unit energy range vs electron trap depth characteristics of the O_2-unexposed and O_2-exposed Alq_3 films are shown in Figs. 4(a) and 4(b), respectively. We obtained the results plotted in these figures from the electron trap depths, which were calculated using results from Figs. 2(a) and 2(b) and eq. (2), and the electron trap concentrations, which were calculated using the differences in the area between neighboring TSC spectra shown in Figs 1(a) and 1(b) and eq. (1),

respectively.[23] We plotted solid curves as references in these figures by fitting the data with a Gaussian-type distribution. We observed two electron trap peaks called peaks (I) and (II) in Fig. 4(a), and one electron trap peak called peak (II) in Fig. 4(b). The maximums of peaks (I) and (II) were located in the range from 0.06 to 0.07 eV and from 0.075 to 0.1 eV, and the width of peak (II) was in the range from 0.06 to 0.07 eV.

Upon comparing Figs. 4(a) and 4(b), we found that peak (II) markedly increased when the Alq_3 films were exposed to O_2 atmosphere, suggesting that electron traps, corresponding to peak (II), originate from O_2 molecules absorbed in the Alq_3 films. We speculate that peak (I) originates from intrinsic electron traps, such as electron traps at grain boundaries.[28,29]

We observed peak (I) only in Fig. 4(a), while there was no peak (I) in Fig. 4(b). Since the number of detrapped electrons from the O_2-exposed Alq_3 film is about one order of magnitude larger than that of detrapped electrons from the O_2-unexposed Alq_3 film, the larger number of detrapped electrons from the O_2-exposed Alq_3 film makes detecting the small peak (I) difficult in the O_2-exposed Alq_3 films.

We observed electron trap peak (II) originating from O_2 molecules in the O_2-unexposed Alq_3 films [Fig. 4(a)], even though we did not expose these Alq_3 films to the O_2 atmosphere before the TSC measurement. We assumed that the cause of this

observation is the contamination of the Alq_3 films by residual O_2 molecules in our vacuum evaporator during film growth.

To verify this hypothesis, we calculated the flux densities (F) of O_2 and Alq_3 molecules striking the substrate surfaces. The F of O_2 molecules striking the substrate surfaces inside a vacuum evaporator can be estimated using an equation obtained from the ideal gas equation and is given by[30)]

$$F = \frac{PN_A^{0.5}}{(2\pi k M_W T)^{0.5}}, \quad (3)$$

where P is the pressure of the gas inside a vacuum evaporator, N_A is Avogadro's number, and M_W is the molecular weight. Assuming that the pressure inside our vacuum evaporator during Alq_3 film growth (10^{-4} Pa) was attributed to the vapor pressure of residual O_2 molecules, the F of O_2 molecules was calculated to be 2.7 x 10^{14} s^{-1} cm^{-2} using Eq. (3) with a P of 10^{-4} Pa, a M_W of 32 g mol^{-1}, and a T of 293 K. Moreover, the F of Alq_3 molecules striking the substrate surfaces during film growth can be estimated using

$$F = \frac{R\rho_V N_A}{M_W}, \quad (4)$$

where R is the deposition rate of Alq_3 and ρ_V is the volume density of Alq_3. We estimated the ρ_V of our vacuum-deposited Alq_3 film to be 1.26 g cm^{-3} using a quartz crystal microbalance installed in our vacuum evaporator and DEKTAK surface

profilometry. The F of Alq_3 molecules during film growth was calculated to be 5.0 x 10^{13} s^{-1} cm^{-2} using eq. (4) with an R of 0.3 nm s^{-1}, a M_W of 459 g mol^{-1}, and a ρ_V of 1.26 g cm^{-3}. When comparing these two Fs, we found that the F of O_2 molecules is five times higher than that of Alq_3 molecules, suggesting that a large density of O_2 molecules, which work as electron traps, contaminated our Alq_3 films during Alq_3 deposition at a background pressure of 10^{-4} Pa.

The electron traps markedly affected the electron current conduction of the Alq_3 films. The J-V characteristics of the O_2-unexposed and O_2-exposed Alq_3 devices are shown in Fig. 5. The driving and turn-on voltages of the O_2-exposed Alq_3 device were higher than those of the O_2-unexposed Alq_3 device. We attribute this to the increase in electron trap concentration caused by the O_2 doping of the Alq_3 films.

Highly dispersive TOF signals and low TOF electron mobilities have been reported in O_2-absorbed Alq_3 films.[3,4] We infer that these previously reported degraded electron transport characteristics are caused by the O_2 trapping effect we demonstrated in this study.

Trap-free space-charge-limited current conduction has been achieved in Alq_3 films prepared under an ultrahigh-vacuum (UHV) condition (10^{-8} Pa) by Kiy *et al.*[22] Although we observed no square law in the J-V characteristics shown in Fig. 5,

preparing the Alq_3 films under an UHV condition must enable the observation of trap-free electron conduction due to a reduction in the *F* of O_2 molecules during Alq_3 film deposition.

4. Conclusions

We measured the TSC spectra and *J*-*V* curves of O_2-unexposed and O_2-exposed Alq_3 films to investigate how O_2 molecules absorbed in Alq_3 films affect electron traps and electron transport. Extensive TSC and *J*-*V* studies revealed that (1) Alq_3 films have an electron trap distribution with peak depths ranging from 0.075 to 0.1 eV and peak widths ranging from 0.06 and 0.07 eV, (2) electron traps originate from O_2 molecules absorbed in the Alq_3 films, and (3) the presence of these O_2 electron traps minimizes electron transport in the Alq_3 films. We emphasize that these findings will help clarify the underlying mechanisms of carrier transport in organic films and improve the *J*-*V* and electroluminescence characteristics of OLEDs.

1) M. A. Lampert and P. Mark: *Current Injection in Solids* (Academic, New York, 1970).

2) P. E. Burrows, Z. Shen, V. Bulovic, D. M. McCarty, S. R. Forrest, J. A. Cronin, and M. E. Thompson: J. Appl. Phys. **79** (1996) 7991.

3) G. G. Malliaras, Y. Shen, D. H. Dunlap, H. Murata, and Z. H. Kafafi: Appl. Phys. Lett. **79** (2001) 2582.

4) H. Fong, K. Lun, and S. So: Jpn. J. Appl. Phys. **41** (2002) L1122.

5) L.-L. Chua, J. Zaumseil, J.-F. Chang, E. C.-W. Ou, P. K.-H. Ho, H. Sirringhaus, and R. H. Friend: Nature (London) **434** (2005) 194.

6) T. Matsushima and C. Adachi: Appl. Phys. Lett. **91** (2007) 103505.

7) C. W. Tang and S. A. VanSlyke: Appl. Phys. Lett. **51** (1987) 913.

8) C. W. Tang, S. A. VanSlyke, and C. H. Chen: J. Appl. Phys. **65** (1989) 3610.

9) C. Adachi, T. Tsutsui, and S. Saito: Appl. Phys. Lett. **57** (1990) 531.

10) S. Naka, H. Okada, H. Onnagawa, Y. Yamaguchi, and T. Tsutsui: Synth. Met. **111-112** (2000) 331.

11) T. Tsutsui: MRS Bull. **22** (1997) No. 39.

12) T. Mizutani, T. Tsukahara, and M. Ikeda: Jpn. J. Appl. Phys. **19** (1980) 2095.

13) H.-E. Tseng, K.-Y. Peng, and S.-A. Chen: Appl. Phys. Lett. **82** (2003) 4086.

14) H.-E. Tseng, C.-Y. Liu, and S.-A. Chen: Appl. Phys. Lett. **88** (2006) 042112.

15) T. Mori, S. Miyake, and T. Mizutani: Jpn. J. Appl. Phys. **34** (1995) 4120.

16) M. Stöβel, J. Staudigel, F. Steuber, J. Simmerer, G. Wittmann, A. Kanitz, H. Klausmann, W. Rogler, W. Roth, J. Schumann, and A. Winnacker: Phys. Chem. Chem. Phys. **1** (1999) 1791.

17) M. Stöβel, J. Staudigel, F. Steuber, J. Simmerer, and A. Winnacker: Appl. Phys. A **68** (1999) 387.

18) S. Barth, U. Wolf, and H. Bässler: Phys. Rev. B **60** (1999) 8791.

19) M. Stöβel, J. Staudigel, F. Steuber, J. Blässing, and J. Simmerer: Appl. Phys. Lett. **76** (2000) 115.

20) M. Stöβel, J. Staudigel, F. Steuber, J. Blässing, J. Simmerer, A. Winnacker, H. Neuner, D. Metzdorf, H.-H. Johannes, and W. Kowalsky: Synth. Met. **111-112** (2000) 19.

21) M. Kiy, I. Biaggio, M. Koehler, and P. Günter: Appl. Phys. Lett. **80** (2002) 4366.

22) M. Kiy, P. Losio, I. Biaggio, M. Koehler, A. Tapponnier, and P. Günter: Appl. Phys. Lett. **80** (2002) 1198.

23) J. Steiger, R. Schmechel, and H. von Seggern: Synth. Met. **129** (2002) 1.

24) N. von Malm, J. Steiger, R. Schmechel, and H. von Seggern: J. Appl. Phys. **89**

(2001) 5559.

25) M. Nakahara, M. Minagawa, T. Oyamada, T. Tadokoro, H. Sasabe, and C. Adachi: Jpn. J. Appl. Phys. **46** (2007) L636.

26) Z. Fang, L. Shan, T. E. Schlesinger, and A. G. Milnes: Mater. Sci. Eng. B **5** (1990) 397.

27) D. C. Look, Z.-Q. Fang, W. Kim, Ö. Aktas, A Botchkarev, A. Salvador, and H. Morkoc: Appl. Phys. Lett. **68** (1996) 3775.

28) A. D. Carlo, F. Piacenza, A. Bolognesi, B. Stadlober, and H. Maresch: Appl. Phys. Lett. **86** (2005) 263501.

29) A. K. Mahapatro, N. Sarkar, and S. Ghosh: Appl. Phys. Lett. **88** (2006) 162110.

30) T. Ikeda, H. Murata, Y. Kinoshita, J. Shike, Y. Ikeda, and M. Kitano: Chem. Phys. Lett. **426** (2006) 111.

Figure captions

Fig. 1. TSC vs sample temperature as functions of T_{STOP} for (a) O_2-unexposed and (b) O_2-exposed Alq_3 thin films.

Fig. 2. Logarithmic TSC vs reciprocal temperature as functions of T_{STOP} for (a) O_2-unexposed and (b) O_2-exposed Alq_3 thin films. Solid lines represent $I_{TSC} \propto \exp(-E_A/kT)$.

Fig. 3. Electron trap depth vs T_{STOP} plots for (a) O_2-unexposed and (b) O_2-exposed Alq_3 thin films.

Fig. 4. Electron trap concentration per unit energy range vs electron trap depth plots for (a) O_2-unexposed and (b) O_2-exposed Alq_3 thin films. Solid curves obtained using Gaussian fitting.

Fig. 5. *J-V* characteristics of O_2-unexposed and O_2-exposed Alq_3 devices with symmetrical MgAg electrodes.

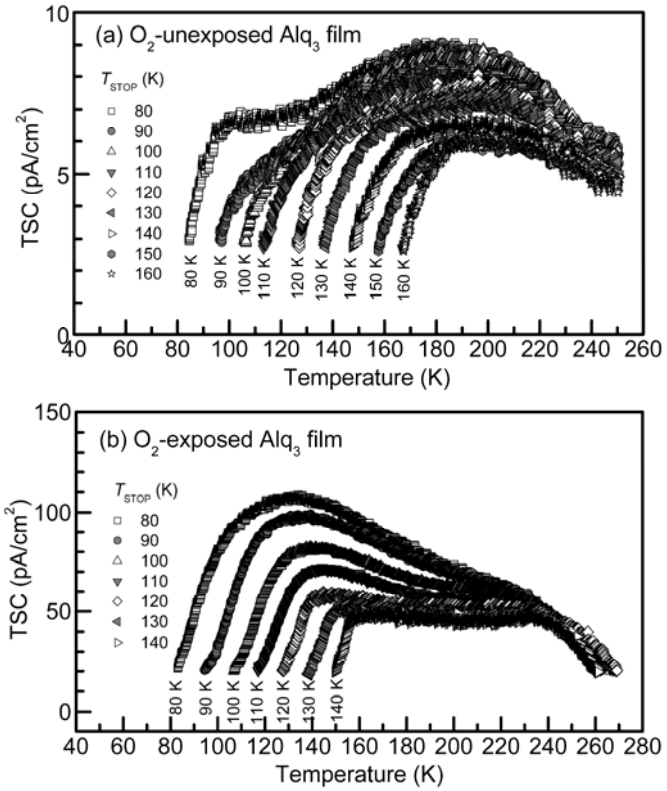

Fig. 1. Toshinori Matsushima and Chihaya Adachi
Japanese Journal of Applied Physics

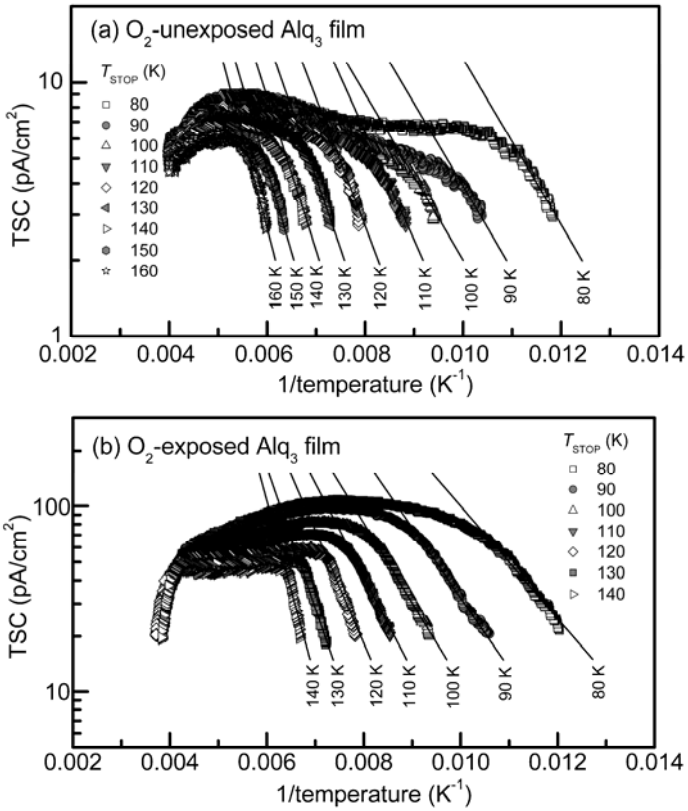

Fig. 2. Toshinori Matsushima and Chihaya Adachi
Japanese Journal of Applied Physics

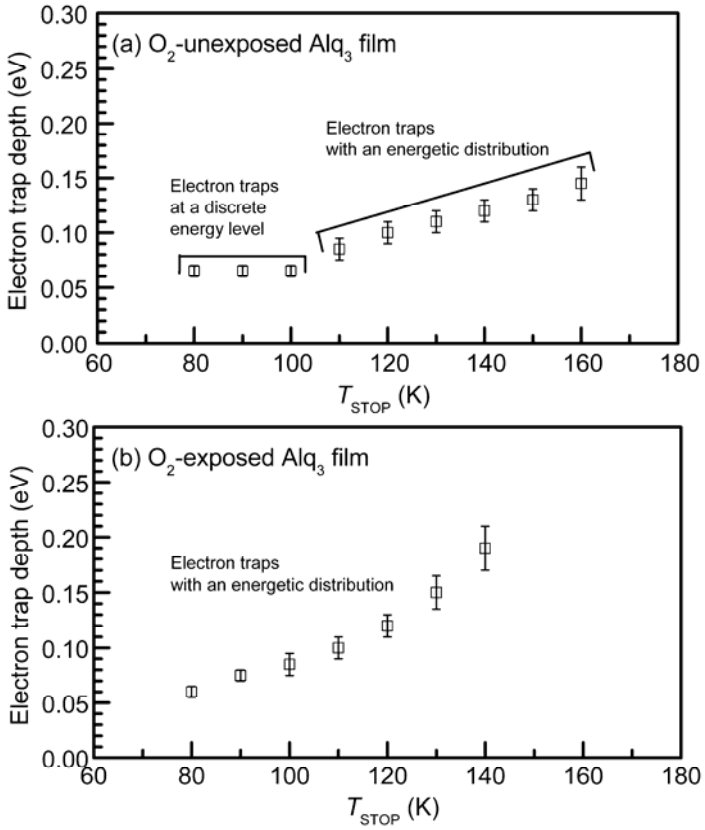

Fig. 3. Toshinori Matsushima and Chihaya Adachi
Japanese Journal of Applied Physics

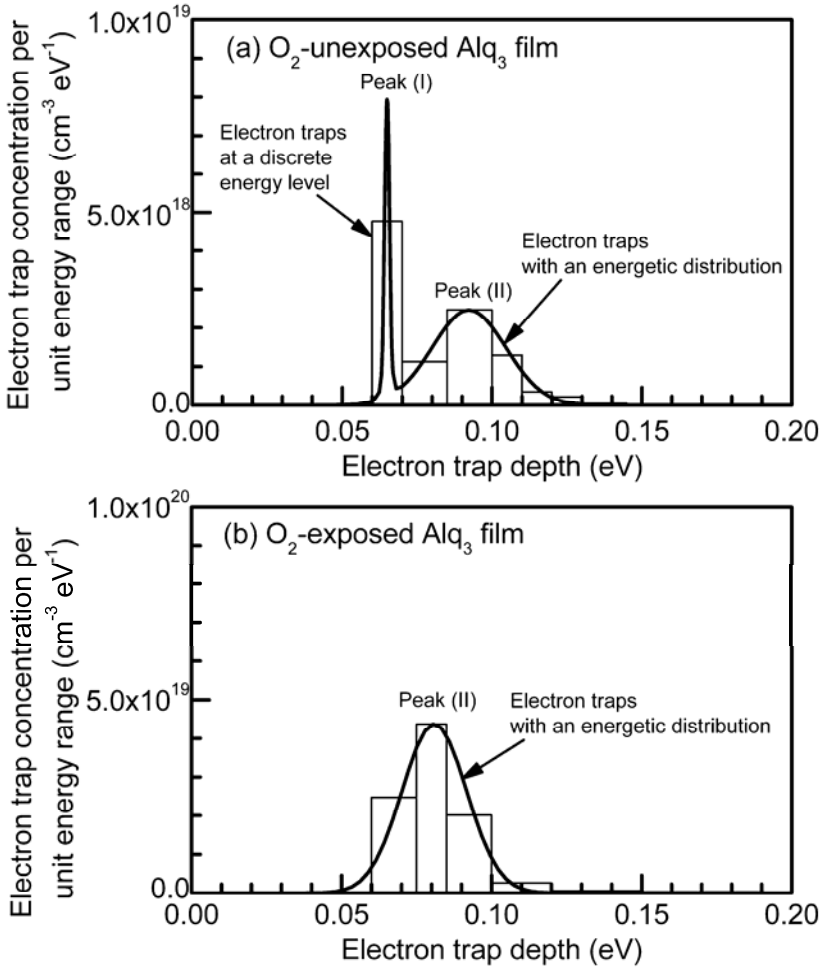

Fig. 4. Toshinori Matsushima and Chihaya Adachi
Japanese Journal of Applied Physics

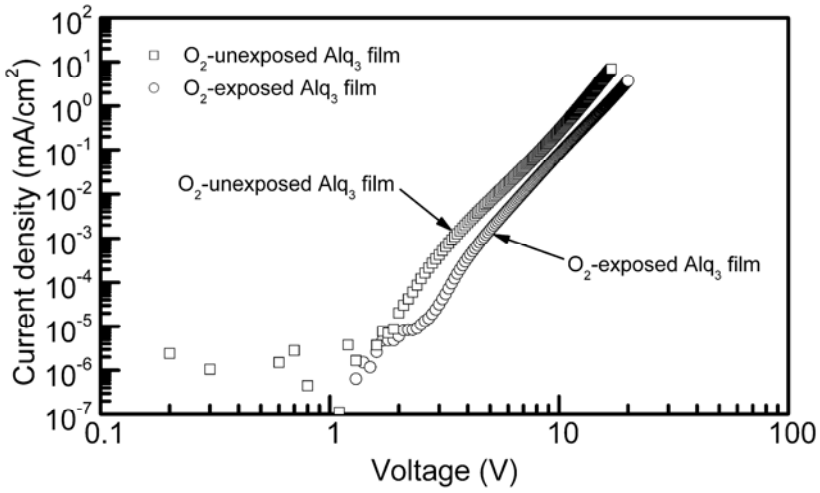

Fig. 5. Toshinori Matsushima and Chihaya Adachi
Japanese Journal of Applied Physics